International Journal of Nanomedicine

Dovepress
open access to scientific and medical research

Open Access Full Text Article

ORIGINAL RESEARCH

Anti-FGFR1 aptamer-tagged superparamagnetic conjugates for anticancer hyperthermia therapy

This article was published in the following Dove Press journal:
International Journal of Nanomedicine
11 April 2017
Number of times this article has been viewed

Przemysław M Jurek*
Konrad Zabłocki*
Urszula Waśko
Maciej P Mazurek
Jacek Otlewski
Filip Jeleń

Department of Protein Engineering, Faculty of Biotechnology, University of Wrocław, Poland

*These authors contributed equally to this work

Abstract: Compounds that recognize and strongly bind to molecular targets are one of the cornerstones of modern pharmaceutics. Work has been ongoing for the past 25 years on the therapeutic use of aptamers, nucleic acid molecules, whose three-dimensional structure is the result of interactions between complementary base pairs. The aptamers selection methods allow the oligonucleotides which bind the molecular target in its native environment to be quickly isolated from a large library of random oligonucleotides. The possibilities presented for aptamers in the field of targeted therapy require the application of effective carriers to counter the renal clearance effect and/or functional cargo to exert therapeutic action if the aptamer is only used as a targeting moiety. Lately, a material gaining ground in biomedical research is iron oxide particles, which exhibit a superparamagnetic characteristic at nanoscale levels. This allows the iron oxide nanoparticles to convert external magnetic energy into heat, a mechanism known as hyperthermy, and efficiently supports conventional oncological treatment. In this study, we describe an experimentally confirmed functional model of targeted anticancer hyperthermia therapy. Using the systematic evolution of ligands by exponential enrichment technique, we selected a DNA aptamer that specifically binds to the extracellular domain of recombinant fibroblast growth factor receptor type-1 (FGFR1) with a nanomolar dissociation constant. The chosen target plays an important role in many crucial cellular processes and is also considered a candidate protein that is involved in tumor initiation, survival and progression. Next, we combined the selected aptamer with iron oxide nanoparticles to produce aptamer superparamagnetic conjugates (ASCs). Finally, we found that targeted ASCs selectively destroy FGFR1-overexpressing human osteosarcoma cells U2OS upon magnetic field irradiation.

Keywords: aptamers, targeted hyperthermia, nanoparticles, iron oxide magnetic nanoparticles, targeted cancer therapy

Abbreviations

ACMF, alternating-current magnetic field; ASCs, aptamer superparamagnetic conjugates; BSA, bovine serum albumin; dsDNA, double-stranded DNA; EMSA, electrophoretic mobility shift assay; FGFR, fibroblast growth factor receptor; FITC, fluorescein isothiocyanate; K_d, dissociation constant; MST, microscale thermophoresis; PBS, phosphate-buffered saline; PCR, polymerase chain reaction; qRT-PCR, quantitative real-time PCR; RT, room temperature; RTKs, receptor tyrosine kinases; SELEX, systematic evolution of ligands by exponential enrichment; SPIONs, superparamagnetic iron oxide nanoparticles; ssDNA, single-stranded DNA.

Introduction

Members of the fibroblast growth factor protein family are involved in various physiological processes, including embryonic growth, angiogenesis and wound healing. They are recognized by FGFRs, a family of transmembrane receptors

Correspondence: Filip Jeleń
Faculty of Biotechnology, University of Wrocław, Fryderyka Joliot-Curie 14a, 50-383 Wrocław, Poland
Email filip.jelen@gmail.com

submit your manuscript | www.dovepress.com
Dovepress
http://dx.doi.org/10.2147/IJN.S125231

classified as RTKs.[1–4] Overexpression of RTKs, along with their constitutive activation, has been reported for numerous tumor types, which makes members of this protein family (and their cognate ligands) promising molecular targets for anticancer therapy.[5] A strong mitogenic effect produced by FGFR stimulation has been observed in fibroblasts, keratinocytes, myoblasts, osteoblasts and endothelial cells (for the latter, angiogenic stimulation has also been observed).[3,6] Overexpression of FGFR has been reported for prostate cancer, thyroid cancer, glioblastoma and bladder cancer.[7–9] Specifically, conditional activation of highly overexpressed FGFR1 is associated with aggressive metastasis and poor prognosis for estrogen receptor-positive lobular breast cancer and small-cell carcinoma, which establishes FGFR1 as an encouraging target for modern anticancer therapies.[10,11]

Although application of magnetism in medicine was described as a novel concept as early as in 1960 by Freeman et al, the real breakthrough in this field was achieved when biological sciences were applied along with dynamically developing nanotechnology.[12] Due to their biophysical characteristics, SPIONs recently became the subject of intensified research in the field of drug delivery methods, diagnostics and anticancer therapies. Unique properties of superparamagnetic nanoparticles suspension result in their ability to absorb the energy of an external ACMF and convert it into heat.[13]

While SPIONs have shown promising results in vitro, the most relevant limitations in their common biomedical usage are their substantial cytotoxicity leading to cell death[14] and iron oxide core agglomeration leading to the loss of superparamagnetism of the nanoparticles. Currently, the most common solution to these problems is a core-shell strategy, which involves coating SPION with organic polymers.[15] Apart from decreasing the cytotoxicity and polydispersion of SPIONs, the polymer shell can increase their biocompatibility and (if chemically modified) can act as a functional group donor for further conjugation procedures.[16–18] The therapeutic mechanism of SPIONs is based on a rapid temperature rise caused by ACMF-exposed superparamagnetic particles. A temperature increase of a few degrees can trigger the apoptotic pathway in cells, which is defined as the magnetic fluid hyperthermia. Its potential in vivo uses, and other iron oxide nanoparticles-related in vivo research, have been thoroughly reviewed elsewhere.[19,20]

However, the limited effectiveness of non-targeted hyperthermia demonstrated by a research group in clinical trials of prostate cancer therapy was caused by an unequal distribution of nanoparticles within the tumor area.[21] The same group has proven the therapeutic safety and effectiveness of magnetic hyperthermia followed by radiotherapy in patients with glioblastoma.[22] Yet, due to the injection method of application, the technique is almost entirely limited to solid tumors. Similar results in the case of small metastatic foci could be obtained by using targeting molecules to allow efficient accumulation of nanoparticles in the vicinity of metastases.

Over the past few years, aptamers – single-stranded oligonucleotides with versatile binding properties – have gained significant attention as targeting molecules. Aptamers have been used successfully to deliver different molecular cargo to target-expressing cells, while discriminating neutral non-target ones.[23–25] The relative ease and speed of their selection using the SELEX technique, their favorable properties (such as reversible denaturation, stability in various conditions, no batch-to-batch variation, ease and low price of large-scale chemical synthesis and versatility of chemical modification) and their effectiveness make aptamers a useful and promising tool for molecular diagnostics, therapeutics and research applications. As shown by Pala et al,[26] a strong and specific targeting DNA aptamer can increase the in vitro efficiency of hyperthermia by requiring over a 90-fold lower nanoparticle concentration for the same lethal effect obtained in a non-targeted fashion.

Combining the aforementioned ideas, we hereby propose a supramolecular conjugate, composed of SPIONs coated with dextran and coupled with an FGFR1-specific aptamer through avidin–biotin interaction (ASCs), for specific recognition and elimination of FGFR1-overexpressing cancer cells in vitro using magnetic field-induced hyperthermia (Figure 1).

Materials and methods

Materials

FGFR1-Fc

Recombinant proteins FGFR1-Fc, FGFR2-Fc, FGFR3-Fc and FGFR4-Fc (based on constructs composed of extracellular domains of FGFRs in fusion with Fc antibody fragment) were prepared as described previously by Doctor Aleksandra Sokolowska-Wedzina (Faculty of Biotechnology, University of Wrocław).[27]

Oligonucleotides

All sequences given throughout the work are denoted from the 5′ to 3′ end.

The library of oligonucleotides was adopted from Pan et al (originally named L8-N30, referred to hereinafter

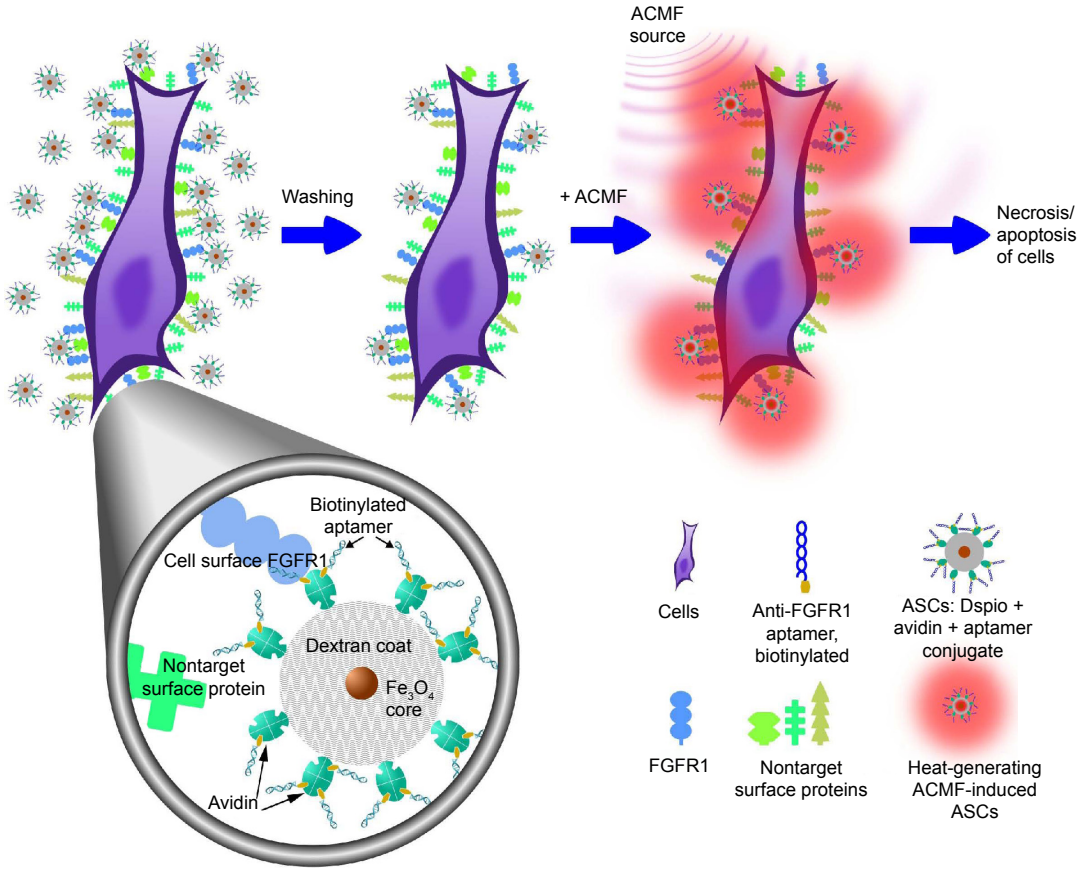

Figure 1 Schematic model of targeted hyperthermia.
Note: The figure shows schematically aptamer-tagged dextran-coated superparamagnetic conjugates (called for brevity aptamer superparamagnetic conjugates or ASCs) specifically binding target-receptors on cell surface and exhibiting hyperthermia upon alternating-current magnetic field (ACMF) induction.
Abbreviation: FGFR1, fibroblast growth factor receptor type-1.

simply as the library),[28] structured as follows: GTA TAC CTG CAG CTG AGG-N_{30}-ATT CGT CTC TAG AGC GCA, where N_{30} denotes a sequence of 30 unbiasedly randomized deoxyribonucleotides. The library was purchased from Integrated DNA Technologies. All other oligonucleotides were purchased from Genomed SA (Warsaw, Poland) (Table S1), including 5′-biotinylated A11-G18T aptamer and a scrambled oligonucleotide of the same length. Biotinylated library was prepared using PCR.

Cell lines

Human osteosarcoma cell line (U2OS) was obtained from American Type Culture Collection (Manassas, VA, USA) and cultured as recommended by the supplier. U2OS cells stably expressing FGFR1 (U2OS-R1) or FGFR3 (U2OS-R3) were a kind gift from Doctor Ellen M Haugsten from the Norwegian Radium Hospital and were grown in Dulbecco's Modified Eagle's Medium supplemented with 10% (v/v) fetal bovine serum, antibiotics (100 U/mL penicillin and 0.1 mg/mL streptomycin) and 0.2 mg/mL geneticin (Thermo Fisher Scientific, Waltham, MA, USA).

Nanomag-Dspio beads

Superparamagnetic polymer-coated iron oxide beads conjugated with avidin (1.5–2.0 µg avidin/mg particle; ~8–9 avidin molecules per particle) (called hereinafter Dspio) were purchased from Micromod Partikeltechnologie GmbH which was supplied as an aqueous dispersion (5 mg/mL). According to the supplier, the mean hydrodynamic particle diameter was in the range of 60–110 nm, consisting of iron oxide crystallite (10–13 nm in diameter) in a matrix of dextran (molecular weight: 40 kDa).

Methods

Cell line verification

The level of FGFR1 expression in U2OS and U2OS-R1 cell lines was monitored by Western blot analysis using specific anti-FGFR1 antibodies. The method used for the preparation

of cell lysate and the protocol of Western blot analysis are included in the Supplementary materials.

Selection of FGFR1-specific aptamers

Selection

FGFR1-specific aptamers were selected from the library using the SELEX procedure in 11 consecutive rounds. Briefly, FGFR1-Fc recombinant protein in PBS (pH 7.4) was immobilized on Protein G-coated magnetic beads (Dynabeads Protein G for Immunoprecipitation; Thermo Fisher Scientific), according to the supplier's instructions. Prior to each round, the ssDNA pool was refolded by heating and snap cooling and incubated with target beads. Next, the beads were washed six times (3× briefly and 3× for 5 min) with selection buffer. Finally, the beads were moved to a fresh tube, the buffer was discarded after the final wash and the beads were resuspended in a small volume of 10 mM Tris–HCl buffer (pH 7.4). Then, the target-bound aptamers were incubated at 95°C for 10 min with vigorous shaking, and the eluate was collected.

At the beginning of rounds 7 and 11, a counter-selection process was performed during which the selection-ready single-stranded aptamer pool was incubated with Fc beads (prepared similarly to FGFR1 beads) for 30 min. Then, the supernatant was collected and used for the subsequent positive selection round. Selection details are presented in Table S2.

Monitoring of amplification and selection process

After each round, the dsDNA product of PCR was immobilized on streptavidin-coated magnetic beads (M-280 Streptavidin Dynabeads; Thermo Fisher Scientific) via a biotinylated primer, and the target-binding non-biotinylated strand was eluted by incubation in freshly prepared 20 mM NaOH. 10× PBS was added to the eluted ssDNA, the pH was adjusted to 7.4 with 1 M NaH_2PO_4, and the sample was used for the subsequent round of selection.

The qRT-PCR performed after each round served to assess the amount of target-eluted ssDNA and to estimate the relative diversity of the oligonucleotide pool by melting curve analysis. The width of the main peak and the melting temperature profile of the product can provide some information on its diversity due to shift caused by non-homologous pairing of different sequence variants in the amplified mixture.[29]

Cloning and sequencing

The amplified target-eluted DNA pool after round 11 was cloned into the pCRII TOPO Vector (TOPO TA Cloning Kit Dual Promoter; Thermo Fisher Scientific) and transformed into *Escherichia coli* DH10 chemically competent cells. Plate-picked single colonies were used to isolate single aptamer clone-containing plasmids (prepared with GeneJET Plasmid Miniprep Kit; Thermo Fisher Scientific), which were subsequently sequenced (LGC Genomics GmbH, Berlin, Germany). Sequences were analyzed using Finch TV software and aligned with the MUSCLE alignment algorithm at Analysis Tool Web Services from European Molecular Biology Laboratory–European Bioinformatics Institute.[30,31]

Aptamer structure analysis and design of mutation variants

Aptamer secondary structure analysis

Selected aptamers were analyzed using the online algorithm NUPACK: Nucleic Acid Package for their predicted secondary structure at 22°C in 137 mM Na^+ and 5 mM Mg^{2+} (matching salt and divalent ion conditions of the selection buffer).[32]

Point mutation design

According to the predicted structure of aptamer A11, several arbitrarily chosen point mutations (one to four bases) were designed, and corresponding oligonucleotides were ordered. Sequences of the designed mutants are presented in Table S3.

Aptamer binding tests

EMSA

Binding of selected aptamers to target and non-target proteins was evaluated by EMSA in a polyacrylamide gel. First, aptamers in PBS were heated for 5 min at 95°C in the presence of 5 mM $MgCl_2$, and the sample was snap-cooled on ice. Next, the samples were left to warm up to RT for 15 min. Then, appropriate analytes (eg, an aptamer and FGFR1-Fc) were mixed in a 10 µL final volume of PBS and incubated for 60 min (if not noted otherwise) at RT. After that, the samples were loaded onto a native 8% polyacrylamide (19:1 acrylamide:bis-acrylamide) gel buffered with Tris-borate-based buffer (containing 44.5 mM Tris–borate and 5 mM $MgCl_2$; pH 8.3) and run in the same buffer in a cold room at 10 V/cm for ~120 min.

MST

K_d values of A11 or A11-G18T aptamers toward FGFR1-Fc were measured in an MST experiment. FGFR1-Fc was labeled with a fluorescent dye through N-hydroxysulfosuccinimide coupling. A serial dilution of non-labeled aptamer was prepared using PBS buffer supplemented with 0.5 mg/mL BSA, 0.05% Tween-20, and 5 mM $MgCl_2$. FGFR1-Fc concentration

was kept constant, whereas the aptamer concentration was varied, starting at the lowest point of 1.53 nM and increasing by a factor of 2 up to 50 µM and 12.5 µM for A11 and A11-G18T, respectively. Ten-microliter samples of appropriate serial dilutions of aptamer were mixed with 10 µL of the fluorescently labeled FGFR1-Fc and loaded into glass capillaries, and the MST analysis was performed using the Monolith NT.115 instrument by courtesy of NanoTemper Technologies GmbH, Germany. The results were analyzed and fitted using NTAffinity Analysis v2.0.

Fluorescence microscopy

U2OS, U2OS-R1 and NIH-3T3 cell lines were grown on microscope cover slides for 24 h at 37°C in full medium. Samples were stained with 2 µM FITC:A11-G18T conjugate, fluorescently labeled with phalloidin and 4′-6-diamidino-2-phenylindole, respectively, and incubated for 1 h in the dark. Then, the slides were rinsed three times with Dulbecco's PBS and treated with 4% paraformaldehyde. Cells were analyzed using a fluorescence microscope at 40×.

Hyperthermia with targeted nanoparticles

Preparation of nanoparticle–aptamer conjugates

One milligram of avidin-coated Dspio particles corresponded to 1.4×10^{12} beads, which were capable of binding ~80 pmol of free biotin (supplier's information). The conjugation step consisted of 2 h incubation of the nanoparticle suspension with two-fold molar excess of biotinylated aptamer, biotinylated random library or biotinylated scrambled oligonucleotide (molar excess calculated as for theoretical maximal binding capacity of the beads). Due to their small size, nanomag-Dspio superparamagnetic nanoparticles could not be separated with a conventional permanent magnet or be centrifuged. Instead, easily removable streptavidin-coated Dynabeads M-280 (2.8 µm in diameter from Thermo Fisher Scientific) were used to remove the unbound oligonucleotides. A magnetic stand was used to pull the Dynabeads to the side of the reaction tube, allowing the supernatant (containing ASCs) to be removed easily for further use. The concentration of ssDNA on ASCs was measured using the Quant-iT OliGreen ssDNA Assay Kit (Thermo Fisher Scientific), and the standard curve was plotted using free A11-G18T-biot aptamer mixed with the same amount of Dspio that was present in the tested sample.

Hyperthermia by targeted nanoparticles

One day prior to hyperthermia experiment, 150,000 cells (either target-expressing U2OS-R1 or control U2OS) were plated on a 35 mm Petri dish and cultured overnight in a full medium. The next day, the medium was enriched with ASCs or bare Dspio solution (final concentration in medium, 0.25 mg/mL) and incubated for 1 h (5% CO_2, 37°C). When indicated (Washing: +), cells were rinsed with PBS three times to remove unbound nanoparticles, resuspended in a complete medium and subjected to an alternating electromagnetic field generated by the induction coil (alternating current, 300 A, 190 kHz; Easyheat; Ambrell, Scottsville, NY, USA) for two 30-min cycles with a 30-min break in between. After the process, the medium was replaced, and the cells were cultured until the next day, when Trypan blue staining was performed, and live cells were counted using a Countess automated cell counter (Thermo Fisher Scientific). The experiment was also performed using bare Dspio nanoparticles (non-targeted fashion) as well as using Dspio conjugated with a pool of random oligonucleotides (denoted as "Lib") or a scrambled oligonucleotide with an irrelevant sequence of the same length instead of the aptamer (denoted as "scrambled") as controls. Results were analyzed, and statistical tests were performed using GraphPad Prism 7.00 software. For the assessment of statistical significance of differences between the samples, a multiple-comparisons test with Tukey's correction was used.

Results

Selection of FGFR1-specific aptamers

We observed an increase in the amount of ssDNA eluted from target beads after successive rounds of SELEX (Table S2 and Figure S1), and a shift and sharpening of the melting curve peak toward higher temperatures of dsDNA produced with qRT-PCR on a target-eluted material (data not shown). These observations suggest an enrichment of the ssDNA pool. Sequencing of 20 single clones after the 11th round showed that all the clones bore almost the same sequence with a few point mutations (sequencing results are presented as aligned sequences in Table S3). EMSA binding tests confirmed that the consensus aptamer A11 selectively binds recombinant FGFR1-Fc (Figures S3 and S4).

Aptamer structure analysis and design of mutation variants

Analysis of aptamer's secondary structure

Predicted secondary structure of the A11 aptamer was obtained using NUPACK online software (Figure 2).

Point mutation design

EMSA analysis of mutants revealed that the majority of changes introduced to the main stem–loop structure (as predicted by NUPACK software) led to the loss of aptamers' target-binding capacity, with the exception of the A11-G18T

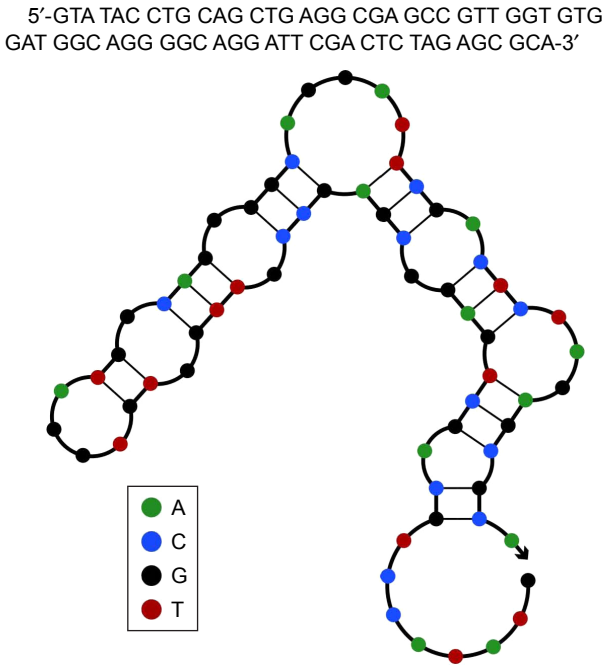

Figure 2 Aptamer A11 predicted structure.
Note: The sequence of A11 aptamer and its two-dimensional structure prediction by NUPACK software, showing distinct stem-loop structure involving both the random region and the primer regions.

mutant (designed for its potentially higher stem stability), which showed an estimated binding strength similar to the wild-type A11 aptamer (Table S4 and Figure S2). The A11-G18T mutant was analyzed using the NUPACK software as described earlier, which showed that the predicted 2D structure was more stable than the original variant A11 by 2.5 kcal/mol.

Aptamer binding tests

EMSA

Gel-shift analysis showed that the A11 aptamer is specific to the extracellular domain of FGFR1 and does not recognize the Fc domain, BSA or any of the other FGFR proteins (extracellular domains of FGFR2–4) (Figures S3 and S4).

MST

Using MST, the K_d values of A11 and A11-G18T aptamers toward FGFR1-Fc were measured to be 1.52 μM ±0.47 μM and 0.237 μM ±0.109 μM, respectively (Figure 3).

Fluorescence microscopy

In vitro binding of the FITC-conjugated A11-G18T aptamer to FGFR1 was clearly confirmed by fluorescent microscopy in naturally expressing FGFR1 NIH-3T3 cell line as well as in stably transfected U2OS-R1 cells, as opposed to the FGFR1-negative U2OS cell line (Figure 4).

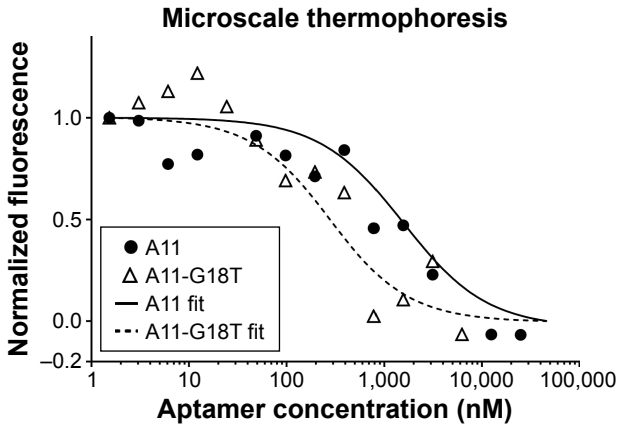

Figure 3 Aptamers binding assessment by microscale thermophoresis.
Notes: Microscale thermophoresis plots obtained for A11 and A11-G18T aptamers toward fluorescently labeled FGFR1-Fc protein. The fluorescence thermoforetic signal was normalized.
Abbreviation: FGFR1, fibroblast growth factor receptor type-1.

Cell lines

Stable FGFR1 expression level in the U2OS-R1 cell line in contrast to FGFR1-negative U2OS cells, was confirmed by Western blotting before each hyperthermia experiment (Figure S5).

Hyperthermia by targeted nanoparticles

Preparation of ASCs

The amount of ssDNA bound on ASCs was measured to be ~24 pmol/mg of Dspio beads, as measured by Quant-iT OliGreen fluorescence-based ssDNA assay. The functional concentration of Dspio beads in the hyperthermia assay was 0.25 mg/mL, which corresponds to 6 nM aptamer concentration.

Magnetic hyperthermia experiments

The results of magnetic fluid hyperthermia experiments showed a highly specific effect of ACMF-exposed receptor-directed ASCs manifested as a decrease of over 40% of viability in U2OS-R1 cell line (Figures 5 and 6). A 20% higher mortality rate was observed only in the positive control – hyperthermia-treated unwashed cells containing 0.25 mg/mL nanoparticle suspension. No statistically significant lethal effect was observed either in the FGFR1-negative U2OS cell line (striped bars, Figure S6) or in the U2OS-R1 cell line targeted by nanoparticles conjugated with a random oligonucleotide library (Lib in Figure 6) of the same length and primer regions as the A11-G18T aptamer. No decrease in viability was found to be caused by the increase in temperature due to the heating of the induction coil, the nanoparticle suspension

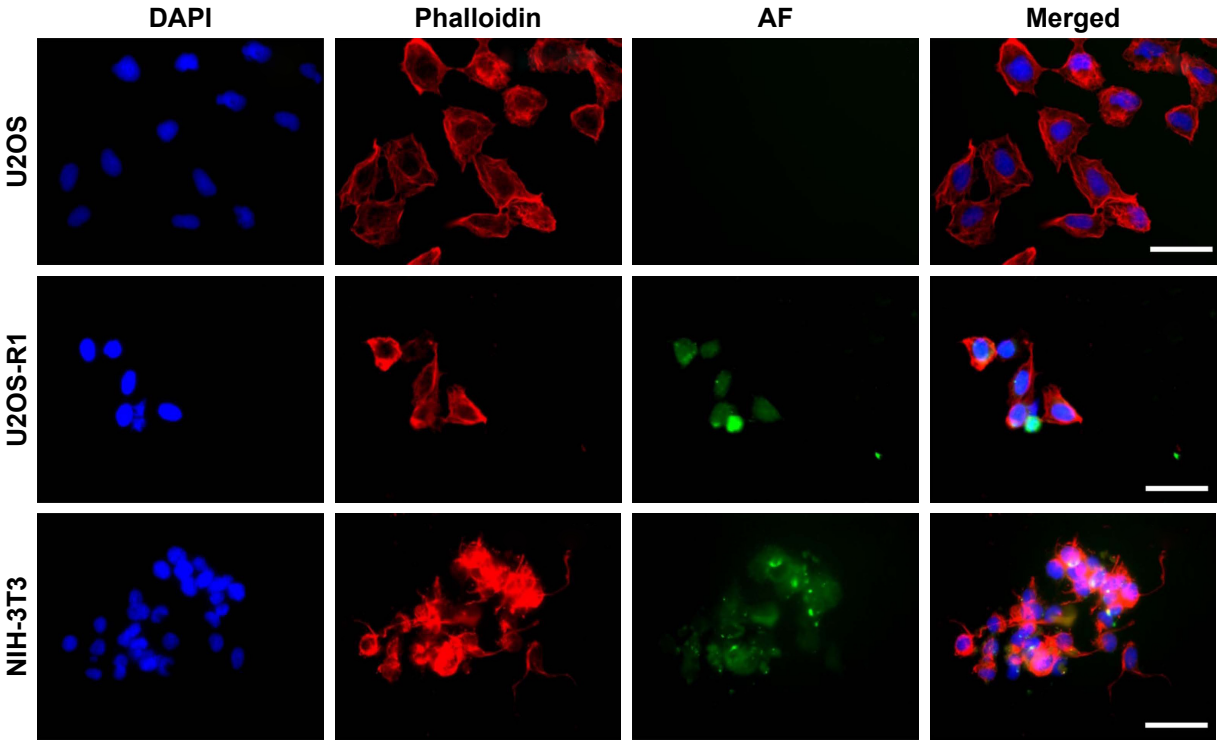

Figure 4 Fluorescence microscopy images of aptamer A11-G18T binding to FGFR1-expressing cells.
Notes: U2OS (upper row), U2OS-R1 (middle row) and NIH-3T3 (lower row) cells were incubated with fluorescein-labeled A11-G18T anti-FGFR1 aptamer, as examined by fluorescence microscopy. Columns from the left: blue DAPI staining of nuclei, red phalloidin staining of actin, green fluorescein signal (staining of surface FGFR1) and a merged picture. Scale bars correspond to 50 μm.
Abbreviations: DAPI, 4′,6-diamidino-2-phenylindole; Phalloidin, fluorescent-labeled phalloidin; AF, FITC-labeled A11-G18T anti-FGFR1 aptamer; FGFR1, fibroblast growth factor receptor type-1; FITC, fluorescein isothiocyanate.

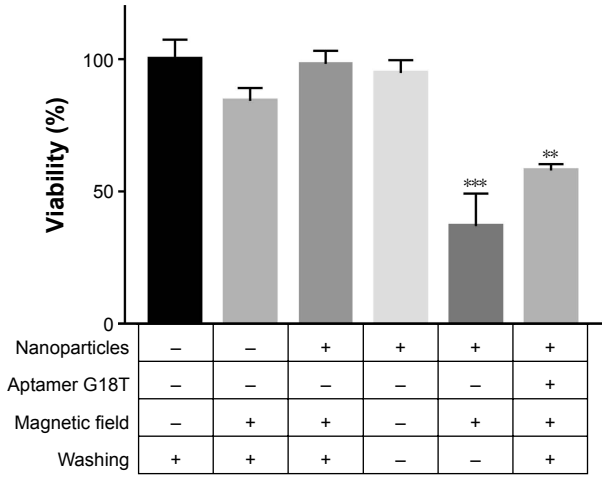

Figure 5 Aptamer-targeted hyperthermia compared to crude unwashed nanoparticles.
Notes: Control experiments for targeted hyperthermia study on USO2-R1 cells. Nontreated cells (washed only; first column) were used as 100% viability control. Samples: columns 2–4 represent different negative controls, while column 5 (+ nanoparticles, + magnetic field) represents a positive control, where Dspio nanoparticles were added to the cells and were not washed before magnetic field application – it shows the maximum killing effect in this setup. The last column shows aptamer-targeted nanoparticles-induced hyperthermia effect. Statistics: ** and *** denote statistically significant difference between the sample and nontreated control (first column) at multiplicity adjusted *P*-values <0.01 and <0.001, respectively. The experiments were performed in duplicate.

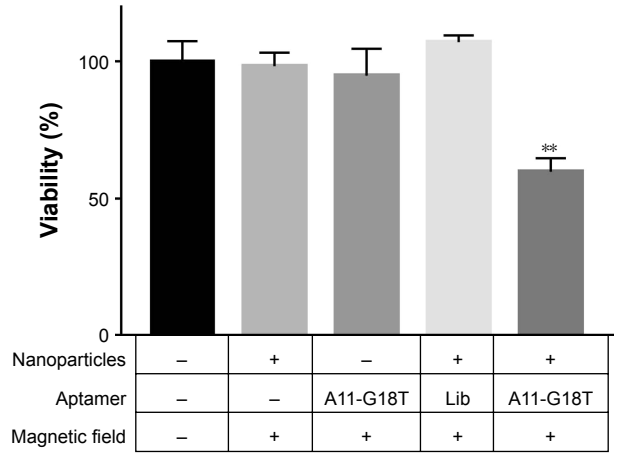

Figure 6 Aptamer-targeted hyperthermia compared to unselected oligonucleotide library.
Notes: Aptamer-targeted hyperthermia study on U2OS-R1 cells. All samples were washed prior to the magnetic field treatment as described in the Methods section. Nontreated cells (first column) were used as 100% viability control. Samples: columns 2–4 represent different negative controls: column 3 (– nanoparticles, + A11-G18T, + magnetic field) validates the effect of free A11-G18T aptamer without the nanoparticles, while column 4 (+ nanoparticles, + Lib, + magnetic field) employs conjugates prepared with unselected randomized oligonucleotide library (Lib) instead of the selected aptamer. The last column shows aptamer-targeted nanoparticles-induced hyperthermia effect. Statistics: **statistically significant difference between the sample and the nontreated control (first column) at multiplicity adjusted *P*-value <0.01. The experiments were performed in duplicate.

itself or the free aptamer A11-G18T. The triple-washing step was sufficient to remove unbound particles, as the washed ACMF-exposed cells were not negatively affected, showing near 100% viability.

Discussion

Selection and optimization of FGFR1-binding aptamer

The selection campaign of aptamers done by the SELEX method provided a specific, FGFR1-binding A11 aptamer, which was further optimized by introduction of a single point mutation to obtain the variant A11-G18T. During the amplification steps, after subsequent rounds of selection, we observed the formation of concatemers. They occurred due to the presence of sequences in the randomized region that are incidentally complementary to the primer regions, and after hybridization, might serve as primers themselves, leading to the formation of nonspecific products. In fact, after several rounds, we observed the concatemers in PCR, the production of which was impossible to avoid by performing fewer cycles. In that case, we decided to purify the DNA of proper length (66 bp) from a denaturing polyacrylamide gel (according to standard procedures), which helped to remove the concatemers, until, surprisingly, they reappeared after several rounds again (data not shown). It is known that these amplification issues can slow down the selection and can lead to the loss of good binders, or even to selection's total failure. The phenomenon of byproduct formation in repetitive PCR during subsequent selection rounds has been analyzed, and an explanation was proposed by Tolle et al.[33] It should be vigilantly addressed during every single SELEX experiment by tight control of amplification conditions.

We also conclude that the selection itself had been conducted for too many rounds. High similarity of the aptamer pool after round 11 suggests that the selection should have been ended at least a couple of rounds earlier, providing more divergent aptamer sequences, and some of them might have presented stronger binding than the consensus sequence A11. Total dominance of the pool by one single clone does not necessarily mean that it is the best possible binder, as SELEX itself imposes biases that cannot be controlled by researchers (such as better amplification of certain sequences during PCR). Therefore, it is strongly advised to closely monitor the selection progress (by means such as assessment of the pool's diversity by melting curve analysis, increase of eluted fraction material or by polyclonal pool binding tests) to finish the enrichment at the right moment.

Nevertheless, the A11 clone proved to be a highly specific FGFR1-binding ligand with a micromolar K_d, and the mutation G18T further improved its K_d by one order of magnitude (down to high nanomolar), possibly by increasing the stability of the double-stranded stem fragment. This is fairly surprising, as the mutated base was positioned in one of the constant flanking regions and not in the randomized selected region. According to the NUPACK secondary structure prediction, however, this G18T mutation closes an opening in one of the stems, which in turn leads to an overall improvement in stability of the whole aptamer (Figure S2). Additional EMSA tests showed that the G18T mutant retained the high specificity of A11 (data not shown), and as its measured K_d was lower than that of A11, it was chosen for further tests. The specificity of A11-G18T, in terms of the ability to discriminate between FGFR1 and the other FGFR variants (Figure S4), has rendered this aptamer useful for further experiments.

Magnetic fluid hyperthermia with targeted ASCs

Although general protocols of in vitro magnetic hyperthermia experiment are well described, a set of preliminary tests was necessary to establish suitable conditions for further research. Hypothetical long-term cytotoxicity of the dextran-coated Dspio nanoparticle suspension was tested, and no such effect was observed (data not shown). The rinsing step after the incubation of cells with ASC solution was carefully optimized. The results confirmed the optimization method, with cell mortality by unwashed ACMF-induced nanoparticles reaching from 50% to 60% (positive control), compared with only a slight decrease in cell viability for a setup including a triple-washing step (Figure 5). Further controls included experiments conducted to exclude the potential negative influence of the A11-G18T aptamer itself on cell viability (Figure 6). Furthermore, high specificity of the targeted therapy was confirmed by testing an unselected library or an arbitrary (scrambled) oligonucleotide, which did not induce any noticeable effect on the U2OS-R1 cells. Despite being selected against FGFR1, the possibility of A11-G18T native cross-reactivity with other FGFR-family members was also examined by using the stably expressing FGFR3 cell line (U2OS-R3) as a control for the ASC hyperthermia experiment (data not shown). No significant decrease in viability was observed, which confirmed the results of the specificity-testing EMSA.

While high hyperthermia specificity was tested by a set of previously described controls, the main experiment confirmed the high therapeutic efficacy of magnetic nanoparticles targeted with the A11-G18T aptamer selected against the extracellular domain of FGFR1. This was achieved by using a relatively low initial nanoparticle concentration

(0.25 mg/mL) as well as low current conditions. In addition, the mortality rate of receptor-expressing cells incubated with ASCs followed by a triple-washing step was merely around 20% lower than the highest achieved mortality for the ACMF-exposed unwashed probe, which indicates high aptamer-mediated targeting efficacy (Figure 5). These results, in combination with all the controls, confirmed that both natively expressed FGFR1 and the targeting A11-G18T are required for an efficient hyperthermia-triggered lethal effect, because the combination that removes the targeting molecule (by using a random oligonucleotide instead of the aptamer or bare nanoparticles) or membrane receptor (by testing the control U2OS non-transfected cell line) does not provide any significant therapeutic effect.

Conclusion

Local hyperthermia induced by magnetic nanoparticles is a promising therapeutic technique, as well as a strategy helping to improve the efficiency of chemotherapy of cancer-suffering patients.[34–37] To increase the localized concentration of the nanoparticles on tumor cells, targeting agents are used, among which nucleic acid aptamers tend to gain more interest.

In this study, we proposed a model for targeted hyperthermia therapy, in which SPIONs covered with a dextran shell were delivered to the surface of the target cells via an FGFR1-binding DNA aptamer selected in our laboratory. The results are convergent with our previous studies,[26] which show that targeted nanoparticles specifically destroy target-expressing cells upon irradiation with an ACMF, while not inflicting any significant damage on control cells.

Acknowledgments

This research was supported by the Wrocław Research Centre EIT+ under the project "Biotechnologies and advanced medical technologies" – BioMed (POIG.01.01.02-02-003/08), which was financed from the European Regional Development Fund (Operational Programme Innovative Economy, 1.1.2).

The authors would like to thank Doctor Aleksandra Sokolowska-Wedzina for the preparation of recombined proteins FGFR1–4, Doctor Anna Serwotka-Suszczak for the collection of fluorescence microscopy images and Doctor Ellen M Haugsten from the Norwegian Radium Hospital for providing us with transfected cell lines.

The authors hereby declare that this study and the use of U2OS, U2OS-R1, and U2OS-R3 cells was reviewed by Doctor Anna Kulma, the Dean's proxy for genetically modified organism committee, and approved by Professor Dorota Nowak, Chair of the Faculty Board and the Dean of the Faculty of Biotechnology, University of Wroclaw.

Disclosure

The authors report no conflicts of interest in this work.

References

1. Kharitonenkov A. FGFs and metabolism. *Curr Opin Pharmacol*. 2009; 9(6):805–810.
2. Ornitz DM. FGFs, heparan sulfate and FGFRs: complex interactions essential for development. *Bioessays*. 2000;22(2):108–112.
3. Tsuboi R, Sato Y, Rifkin DB. Correlation of cell migration, cell invasion, receptor number, proteinase production, and basic fibroblast growth factor levels in endothelial cells. *J Cell Biol*. 1990;110(2): 511–517.
4. Eswarakumar VP, Lax I, Schlessinger J. Cellular signaling by fibroblast growth factor receptors. *Cytokine Growth Factor Rev*. 2005; 16(2):139–149.
5. Regulska K, Stanisz B, Regulski M. Indywidualizacja terapii przeciwnowotworowej; molekularne uwarunkowania mechanizmów dzia\lania nowoczesnych leków onkologicznych [Individualization of anticancer therapy; molecular targets of novel drugs in oncology]. *Postepy Hig Med Dosw (Online)*. 2012;66:855–867. Polish [with English abstract].
6. Xian W, Schwertfeger KL, Vargo-Gogola T, Rosen JM. Pleiotropic effects of FGFR1 on cell proliferation, survival, and migration in a 3D mammary epithelial cell model. *J Cell Biol*. 2005;171(4): 663–673.
7. Katoh M, Nakagama H. FGF receptors: cancer biology and therapeutics. *Med Res Rev*. 2014;34(2):280–300.
8. Kondo T, Zheng L, Liu W, Kurebayashi J, Asa SL, Ezzat S. Epigenetically controlled fibroblast growth factor receptor 2 signaling imposes on the RAS/BRAF/mitogen-activated protein kinase pathway to modulate thyroid cancer progression. *Cancer Res*. 2007;67(11):5461–5470.
9. Chaffer CL, Dopheide B, Savagner P, Thompson EW, Williams ED. Aberrant fibroblast growth factor receptor signaling in bladder and other cancers. *Differentiation*. 2007;75(9):831–842.
10. Reis-Filho JS, Simpson PT, Turner NC, et al. FGFR1 emerges as a potential therapeutic target for lobular breast carcinomas. *Clin Cancer Res*. 2006;12(22):6652–6662.
11. Schröck A, Göke F, Wagner P, et al. Fibroblast growth factor receptor-1 as a potential therapeutic target in sinonasal cancer. *Head Neck*. 2014;36(9):1253–1257.
12. Freeman MW, Arrott A, Watson JHL. Magnetism in medicine. *J Appl Phys*. 1960;31(5):S404–S405.
13. Laurent S, Dutz S, Häfeli UO, Mahmoudi M. Magnetic fluid hyperthermia: focus on superparamagnetic iron oxide nanoparticles. *Adv Colloid Interface Sci*. 2011;166(1–2):8–23.
14. Yu M, Huang S, Yu KJ, Clyne AM. Dextran and polymer polyethylene glycol (PEG) coating reduce both 5 and 30 nm iron oxide nanoparticle cytotoxicity in 2D and 3D cell culture. *Int J Mol Sci*. 2012; 13(5):5554–5570.
15. Sungwook H, Yongmin C, Ilsu R. Chitosan-coated ferrite (Fe_3O_4) nanoparticles as a T2 contrast agent for magnetic resonance Imaging. *J Korean Phys Soc*. 2010;56(3):868–873.
16. Thomas R, Park I-K, Jeong Y. Magnetic iron oxide nanoparticles for multimodal imaging and therapy of cancer. *Int J Mol Sci*. 2013; 14(8):15910–15930.
17. Yang J, Luo Y, Xu Y, et al. Conjugation of iron oxide nanoparticles with RGD-modified dendrimers for targeted tumor MR imaging. *ACS Appl Mater Interfaces*. 2015;7(9):5420–5428.
18. Xu H, Aguilar ZP, Yang L, et al. Antibody conjugated magnetic iron oxide nanoparticles for cancer cell separation in fresh whole blood. *Biomaterials*. 2011;32(36):9758–9765.
19. Valdiglesias V, Fernández-Bertólez N, Kiliç G, et al. Are iron oxide nanoparticles safe? Current knowledge and future perspectives. *J Trace Elem Med Biol*. 2016;38:53–63.

20. Beik J, Abed Z, Ghoreishi FS, et al. Nanotechnology in hyperthermia cancer therapy: from fundamental principles to advanced applications. *J Control Release*. 2016;235:205–221.
21. Johannsen M, Thiesen B, Wust P, Jordan A. Magnetic nanoparticle hyperthermia for prostate cancer. *Int J Hyperthermia*. 2010; 26(8):790–795.
22. Maier-Hauff K, Ulrich F, Nestler D, et al. Efficacy and safety of intratumoral thermotherapy using magnetic iron-oxide nanoparticles combined with external beam radiotherapy on patients with recurrent glioblastoma multiforme. *J Neurooncol*. 2011;103(2):317–324.
23. Azhdarzadeh M, Atyabi F, Saei AA, et al. Theranostic MUC-1 aptamer targeted gold coated superparamagnetic iron oxide nanoparticles for magnetic resonance imaging and photothermal therapy of colon cancer. *Colloids Surf B Biointerfaces*. 2016;143:224–232.
24. Zhao N, Pei S-N, Qi J, et al. Oligonucleotide aptamer-drug conjugates for targeted therapy of acute myeloid leukemia. *Biomaterials*. 2015; 67:42–51.
25. Wen J, Tao W, Hao S, Iyer SP, Zu Y. A unique aptamer-drug conjugate for targeted therapy of multiple myeloma. *Leukemia*. 2016;30(4): 987–991.
26. Pala K, Serwotka A, Jeleń F, Jakimowicz P, Otlewski J. Tumor-specific hyperthermia with aptamer-tagged superparamagnetic nanoparticles. *Int J Nanomedicine*. 2014;9:67–76.
27. Sokolowska-Wedzina A, Borek A, Chudzian J, Jakimowicz P, Zakrzewska M, Otlewski J. Efficient production and purification of extracellular domain of human FGFR-Fc fusion proteins from Chinese hamster ovary cells. *Protein Expr Purif*. 2014;99:50–57.
28. Pan W, Xin P, Clawson GA. Minimal primer and primer-free SELEX protocols for selection of aptamers from random DNA libraries. *Biotechniques*. 2008;44(3):351–360.
29. Schutze T, Arndt PF, Menger M, et al. A calibrated diversity assay for nucleic acid libraries using DiStRO – a Diversity Standard of Random Oligonucleotides. *Nucleic Acids Res*. 2010;38(4):e23.
30. McWilliam H, Li W, Uludag M, et al. Analysis Tool Web Services from the EMBL-EBI. *Nucleic Acids Res*. 2013;41(Web Server issue): W597–W600.
31. Edgar RC. MUSCLE: a multiple sequence alignment method with reduced time and space complexity. *BMC Bioinformatics*. 2004;5:113.
32. Zadeh JN, Steenberg CD, Bois JS, et al. NUPACK: analysis and design of nucleic acid systems. *J Comput Chem*. 2011;32(1):170–173.
33. Tolle F, Wilke J, Wengel J, Mayer G. By-product formation in repetitive PCR amplification of DNA libraries during SELEX. *PLoS One*. 2014;9(12):e114693.
34. Sato A, Itcho N, Ishiguro H, et al. Magnetic nanoparticles of Fe3O4 enhance docetaxel-induced prostate cancer cell death. *Int J Nanomedicine*. 2013;8:3151–3160.
35. Quinto CA, Mohindra P, Tong S, Bao G. Multifunctional superparamagnetic iron oxide nanoparticles for combined chemotherapy and hyperthermia cancer treatment. *Nanoscale*. 2015;7(29):12728–12736.
36. Aljarrah K, Mhaidat NM, Al-Akhras M-AH, et al. Magnetic nanoparticles sensitize MCF-7 breast cancer cells to doxorubicin-induced apoptosis. *World J Surg Oncol*. 2012;10:62.
37. Silva AC, Oliveira TR, Mamani JB, et al. Application of hyperthermia induced by superparamagnetic iron oxide nanoparticles in glioma treatment. *Int J Nanomedicine*. 2011;6:591–603.